Nanometer-scale scanning sensors fabricated using stencil lithography

A. R. Champagne, A. J. Couture, F. Kuemmeth, and D. C. Ralph[a)]
Laboratory of Atomic and Solid State Physics, Cornell University, Ithaca New York 14853

(Received 5 November 2002; accepted 2 January 2003)

We describe a flexible technique for fabricating 10-nm-scale devices for use as high-resolution scanning sensors and functional probes. Metallic structures are deposited directly onto atomic force microscope tips by evaporation through nanoscale holes fabricated in a stencil mask. We report on the lithographic capabilities of the technique and discuss progress in one initial application, to make high-spatial-resolution magnetic force sensors. © *2003 American Institute of Physics.*
[DOI: 10.1063/1.1554483]

Advanced forms of scanning-probe microscopy (SPM) have recently been introduced that employ nanofabricated structures that serve as scanning sensors or "functional" probes. Examples include scanning thermal microscopy,[1] gated scanning-tunneling microscopy (STM),[2] and electrometry with scanning single-electron transistors.[3] In order to achieve high sensitivity and spatial resolution, functional SPM probes must be built near the apex of a tip so as to be scanned close to the sample surface. The fabrication of devices on the curved surface of a tip presents a challenge since standard lithographic processes require flat substrates. Previously-employed techniques for making structures on scanning-probe tips[2–4] have difficulties controlling feature sizes below 100 nm. Here, we report on a lithographic procedure employing stencil masks, which enables the fabrication of a wide variety of devices at the apex of atomic force microscope (AFM) tips with spatial resolution controllable down to 10 nm. We also describe a specific application of the technique: to fabricate high spatial resolution magnetic force microscopy (MFM) tips.

The initial step in our fabrication process is to make a stencil mask by etching nanoscale holes through a silicon nitride membrane.[5,6] We first make suspended membranes of silicon nitride 50 nm thick and 50–100 μm wide using photolithography and etching in a KOH solution to remove selected portions of a silicon substrate. Electron-beam lithography is then employed to write the desired pattern on the membrane. Holes are etched through the membrane using reactive ion etching with CHF_3/O_2 plasma. The hole diameter can be made as small as 5 nm.[6] We generally employ somewhat larger holes to avoid premature clogging during the metal depositions.

Once the desired stencil membrane is fabricated, it is mounted beneath a commercial AFM tip in a custom-built, vacuum-compatible, AFM system,[7] and coarse alignment is achieved using optical microscopy. The AFM assembly is then placed inside an evaporation chamber (base pressure 10^{-8} Torr). Figure 1(a) shows the geometry for the pattern-transfer process. For convenience in operation under vacuum conditions, our AFM utilizes a quartz tuning fork [Fig. 1(b)] to sense the distance between the tip and the surface.[8–10] The procedure for gluing the tip to the tuning fork allows the tip to be removed easily following metal deposition, so that we can use the modified tip later in any SPM machine.

While under vacuum, but before beginning the process of metal deposition, we are able to align the position of the tip relative to the stencil pattern by simply imaging the pattern with the AFM. Figure 1(c) shows a scan on a stencil mask obtained with our microscope under vacuum, showing a pattern of five narrow, line-shaped holes ($\approx$30 nm wide) etched through the stencil. Just before the pattern transfer, the tip is positioned directly over the desired hole and retracted 80–100 nm from the surface to prevent contact between the tip and stencil during the evaporation. The evaporation rate used is generally $\sim$5 Å/s.

In Fig. 2, we show scanning electron microscope (SEM) images of test structures deposited on the apex of AFM tips, illustrating the resolution of the stencil technique. Due to the limited depth of focus of SEMs, it is difficult to image structures deposited on the sharp apex of commercial AFM tips. Therefore, we purposely blunted the tips used for Fig. 2 before metal deposition to radii of $\sim$50–300 nm, in order to provide a somewhat more uniform surface for imaging. We achieved the blunting by etching the tips in a SF_6/O_2 plasma followed by deposition of 100 nm of SiO_2. Figure 2(a) shows a five$\times$five array of 20-nm-diameter erbium dots deposited at the apex of a tip. We selected erbium as our depo-

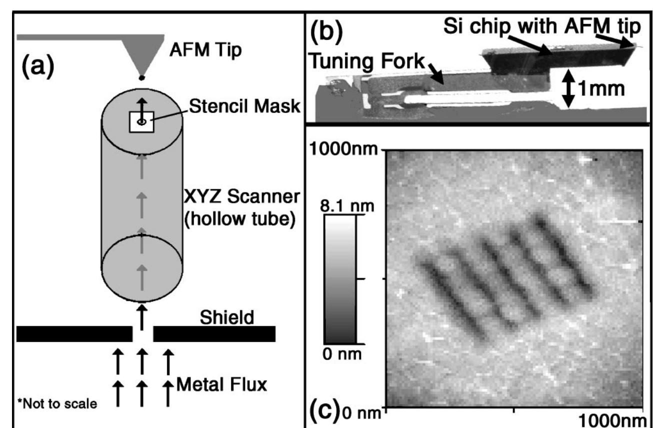

FIG. 1. (a) Schematic diagram of the deposition geometry (not to scale). Metal is deposited from the source, through holes in the stencil membrane, onto the AFM tip. (b) Picture of a commercial AFM tip mounted on a tuning fork used for sensing the tip–surface interaction. (c) AFM image of a pattern of holes in a stencil membrane, acquired prior to deposition.

[a)]Electronic mail: ralph@comr.cornell.edu

0003-6951/2003/82(7)/1111/3/$20.00

© 2003 American Institute of Physics
Downloaded 14 Mar 2003 to 128.84.231.230. Redistribution subject to AIP license or copyright, see http://ojps.aip.org/aplo/aplcr.jsp

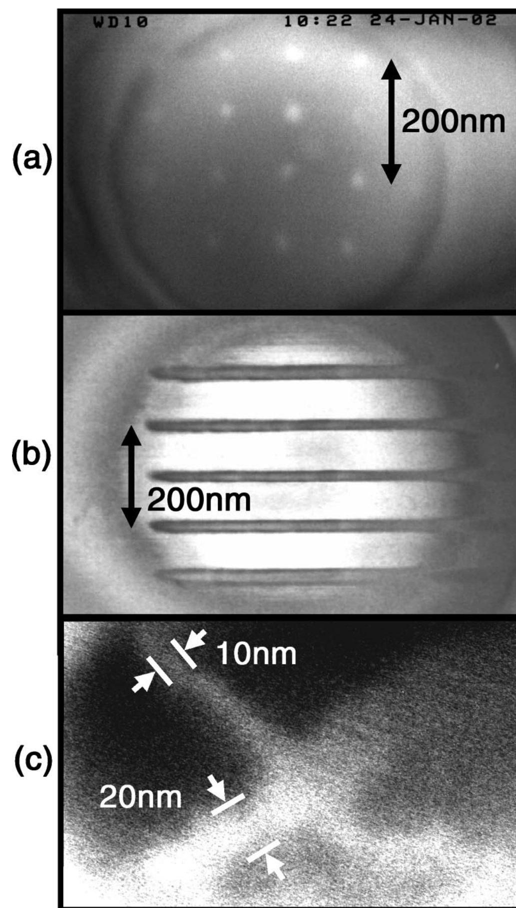

FIG. 2. Examples of test patterns made by depositing metal on AFM tips. (a) A 5×5 array of 20-nm-diameter erbium dots. (b) A pattern of five 20-nm-wide Er lines. (c) Two aligned layers of lithography at the end of one AFM tip, a 20-nm-wide Er line crossing a 10-nm-wide line.

sition layer for these test samples because it offers a good contrast in electron microscopy and sticks well to the tip. The interdot spacing in Fig. 2(a) is 100 nm and a thickness of 50 nm of metal was evaporated. According to a previous study[6] it is possible to deposit a thickness of Er about 1.5 times the diameter of the holes etched in the stencil mask before these clog; thus we expect that the holes in the stencil used for Fig. 2(a) became clogged during the deposition. Figure 2(b) shows a pattern of five Er lines 20 nm wide and 400 nm long deposited on another tip. The line spacing is 100 nm and the thickness deposited is 40 nm. The features in Figs. 2(a) and 2(b) are sharp down to a few nanometers, indicating minimal drift of the tip during the evaporation.

In Fig. 2(c), we show a SEM image demonstrating our ability to align two separate layers of lithography on the same AFM tip, a procedure that can be required to make complex devices. First we deposited the 20-nm-wide, 30-nm-thick Er line using the procedure described above. Without breaking vacuum, we then repositioned the AFM tip over a perpendicular line-shaped hole etched in the same silicon nitride membrane and deposited the 10-nm-wide Er line at a right angle to the previous one. The second line-shaped hole is narrowed from its original width of 40 nm due to partial clogging during the first evaporation. Only a short section of the lines are displayed in Fig. 2(c) due to the rounding of the tip (radius <100 nm).

As a first application of the stencil technique for making

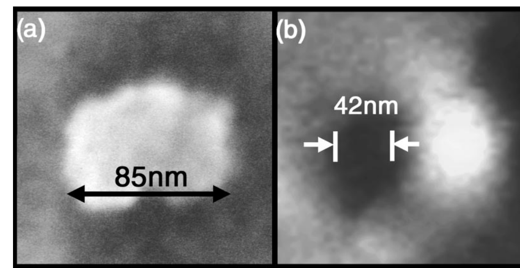

FIG. 3. (a) SEM image of a cobalt nanopillar used for testing our MFM resolution. (b) MFM image of a nanopillar acquired with a stencil-deposited CoCr dot at the end of an AFM tip.

functional SPM probes, we have deposited magnetic nanostructures on tips to serve as high-spatial-resolution MFM sensors. Typically, commercial MFM tips are coated with a continuous ferromagnetic film. However, both the spatial resolution of MFM and the degree to which magnetic samples are perturbed by the tip can be improved by limiting the magnetic material to a small volume near the apex of the tip.[11] It has been shown that tips with a magnetic dot as large as 500 nm have an improved spatial resolution compared to similar tips coated with a continuous film.[12] A variety of different strategies have been pursued to make improved-resolution MFM tips,[11–17] and the best clearly-demonstrated spatial resolution is, to our knowledge, a full width at half maximum (FWHM) of 37 nm in two dimensions[14] and about 30 nm in one dimension.[17]

We deposited single dots of 90% Co/10% Cr alloy ranging in diameter from 140 to 25 nm at the end of sharp (unblunted) AFM tips using the stencil technique. We used commercially available tips[18] with a resonant frequency of 160 kHz and a spring constant of 5 N/m. We chose these relatively stiff cantilevers compared to the state-of-the-art[19] because we performed our MFM testing in air, and therefore needed to avoid having capillary forces from adsorbed water disrupt the MFM imaging.[20] We found that the stiffness of the cantilever limited our force gradient sensitivity so that we could not sense magnetic signals with our smallest deposited structures. The use of floppier cantilevers in vacuum would be necessary to test the full capabilities of the stencil technique. Nevertheless, even with relatively large deposited structures, our magnetic-dot tips exhibited resolution comparable to the best results reported previously.[14]

In order to test the performance of the MFM tips, we imaged 10-nm-thick cobalt nanopillars with dimensions of 85×60 nm [Fig. 3(a)].[21] Figure 3(b) displays a magnetic phase contrast image of the magnetic dipole signal from one nanopillar, obtained using a tip with a stencil-fabricated, 140-nm-diameter CoCr dot, deposited with a normal-incidence thickness of 50 nm on the end of a tip with a nominal radius of curvature of 20 nm. The tip–sample spacing during the MFM imaging was approximately 25 nm. The FWHM resolution in Fig. 3(a) is 42 nm, limited by the lateral extent of the magnetic source. With commercial MFM tips,[22] we achieved FWHM resolution of 60 nm.

The main advantage of the stencil technique over other approaches is that even better performance is possible. By using cantilevers with smaller spring constants, the force gradient sensitivity can be enhanced by as much as a factor of 1000,[19,23] meaning that magnetic dots potentially as small as

Downloaded 14 Mar 2003 to 128.84.231.230. Redistribution subject to AIP license or copyright, see http://ojps.aip.org/aplo/aplcr.jsp

10 nm, approaching the paramagnetic limit, might be used as MFM sensors. Furthermore, because the stencil allows us to pattern the shape of the deposited metal down to the 10-nm scale, the magnetic structure of the tip could be controlled to be a well-oriented dipole, making quantitative analysis of MFM images more straightforward. The stencil technique also has the potential to produce many other types of functional SPM tips. We anticipate being able to make both gated-STM tips and scanning single-electron transistors with pattern definitions close to 10 nm.[2,3] This would greatly increase the sample-gate coupling in gated STM, and would allow operation of scanning single-electron transistors at temperatures well above 1 K.[3] Other applications are also imaginable, including improved near-field optical probes.[24]

In summary, we have developed a lithographic process that allows the deposition of metal nanostructures with a resolution down to 10 nm directly onto SPM tips. We have also shown that multiple layers of lithography can be deposited and aligned. The process offers the possibility to build many types of high resolution scanning sensors and functional SPM probes.

The authors wish to thank C. Daugherty, M. M. Deshmukh, J. R. Petta, E. B. Myers, and A. N. Pasupathy. This work was funded by the Packard Foundation and the NSF (ECS-0080393 and through use of the Cornell Nanofabrication Facility/NNUN).

[1] D. G. Cahill, K. Goodson, and A. Majumdar, J. Heat Transfer **124**, 223 (2002).
[2] L. Gurevich, L. Canali, and L. P. Kouwenhoven, Appl. Phys. Lett. **76**, 384 (2000).
[3] M. J. Yoo, T. A. Fulton, H. F. Hess, R. L. Willett, L. N. Dunkleberger, R. J. Chichester, L. N. Pfeiffer, and K. W. West, Science **276**, 579 (1997).
[4] H. Zhou, G. Mills, B. K. Chong, A. Midha, L. Donaldson, and J. M. R. Weaver, J. Vac. Sci. Technol. A **17**, 2233 (1999).
[5] K. S. Ralls, R. A. Buhrman, and R. C. Tiberio, Appl. Phys. Lett. **55**, 2459 (1989).
[6] M. M. Deshmukh, D. C. Ralph, M. Thomas, and J. Silcox, Appl. Phys. Lett. **75**, 1631 (1999).
[7] A. R. Champagne, A. J. Couture, and D. C. Ralph (unpublished).
[8] K. Karrai and R. D. Grober, Appl. Phys. Lett. **66**, 1842 (1995).
[9] H. Edwards, L. Taylor, W. Duncan, and A. J. Melmed, J. Appl. Phys. **82**, 980 (1997).
[10] R. D. Grober, J. Acimovic, J. Schuck, D. Hessman, P. J. Kindlemann, J. Hespanha, A. S. Morse, K. Karrai, I. Tiemann, and S. Manus, Rev. Sci. Instrum. **71**, 2776 (2000).
[11] U. Hartmann, Annu. Rev. Mater. Sci. **29**, 53 (1999).
[12] S. H. Liou, IEEE Trans. Magn. **35**, 3989 (1999).
[13] P. B. Fischer, M. S. Wei, and S. Y. Chou, J. Vac. Sci. Technol. B **11**, 2570 (1993).
[14] G. D. Skidmore and E. Dan Dahlberg, Appl. Phys. Lett. **71**, 3293 (1997).
[15] T. Arie, H. Nishijima, S. Akita, and Y. Nakayama, J. Vac. Sci. Technol. A **18**, 104 (2000).
[16] L. Folks, M. E. Best, P. M. Rice, B. D. Terris, D. Weller, and J. N. Chapman, Appl. Phys. Lett. **76**, 909 (2000).
[17] G. N. Phillips, M. Siekman, L. Abelmann, and J. C. Lodder, Appl. Phys. Lett. **81**, 865 (2002).
[18] MikroMash, Non-contact silicon cantilever NSC14.
[19] H. J. Mamin and D. Rugar, Appl. Phys. Lett. **79**, 3358 (2001).
[20] D. A. Grigg, P. E. Russell, and J. E. Griffith, J. Vac. Sci. Technol. A **10**, 680 (1992).
[21] S. Evoy, D. W. Carr, L. Sekaric, Y. Suzuki, J. M. Parpia, and H. G. Craighead, J. Appl. Phys. **87**, 404 (2000).
[22] Nanoprobe SPM tips, MESP 66–83 KHz.
[23] The force gradient sensivity of a cantilever is proportional to $\sqrt{k/Q\omega}$, where k is the spring constant, Q is the quality factor, and ω is the resonant frequency of the cantilever.
[24] R. D. Grober, R. J. Schoelkopf, and D. E. Prober, Appl. Phys. Lett. **70**, 1354 (1997).

Downloaded 14 Mar 2003 to 128.84.231.230. Redistribution subject to AIP license or copyright, see http://ojps.aip.org/aplo/aplcr.jsp